*Acta Biochim Biophys Sin*, 2016, 48(2), 145–152
doi: 10.1093/abbs/gmv121
Advance Access Publication Date: 18 December 2015
Original Article

Original Article

# A SIRT4-like auto ADP-ribosyltransferase is essential for the environmental growth of *Mycobacterium smegmatis*

**Yongcong Tan[1,†], Zhihong Xu[1,†], Jing Tao[1], Jinjing Ni[1], Wei Zhao[2], Jie Lu[3], and Yu-Feng Yao[1,*]**

[1]Laboratory of Bacterial Pathogenesis, Department of Microbiology and Immunology, Institutes of Medical Sciences, Shanghai Jiao Tong University School of Medicine, Shanghai 200025, China, [2]Laboratory of Synthetic Biology, Institute of Plant Physiology and Ecology, Shanghai Institutes for Biological Sciences, Chinese Academy of Sciences, Shanghai 200032, China, and [3]Department of Infectious Diseases, Shanghai Ruijin Hospital, Shanghai 200025, China

[†]These authors contributed equally to this work.
*Correspondence address. Tel/Fax: +86-21-64671226; E-mail: yfyao@sjtu.edu.cn

Received 6 September 2015; Accepted 26 September 2015

## Abstract

SIRT family proteins are highly conserved both in the structure and function among all the organisms, and are involved in gene silencing, DNA damage repair, cell growth and metabolism. Here, a SIRT4 homologue MSMEG_4620 was identified and characterized in *Mycobacterium smegmatis*. MSMEG_4620 exhibits deacetylase activity that can be activated by fatty acids. Interestingly, MSMEG_4620 also possesses auto ADP-ribosylation activity. MSMEG_4620 is modified on arginine residues as revealed by a chemical stability assay. Moreover, the auto ADP-ribosylation activity of MSMEG_4620 was found to be enhanced by ferric ion. Notably, the SIRT4 homologues are widely distributed in the genomes of environmental mycobacterial species instead of pathogenic mycobacterial species. When *MSMEG_4620* was deleted in *M. smegmatis*, the mutant strain showed a growth defect in 7H9 minimal medium compared with the parental strain. Taken together, these results provided the characteristics of a SIRT4 homologue in prokaryotes and implicated its critical roles in the growth of environmental mycobacterial species.

**Key words**: MSMEG_4620, auto ADP-ribosylation, deacetylation, SIRT4, environmental mycobacteria

## Introduction

SIRT family proteins, commonly named as sirtuins, are homologous to the yeast transcriptional repressor Sir2p. Sirtuins can utilize $NAD^+$ as a cofactor and deacetylate a wide variety of substrates, thereby regulating almost all life processes including aging [1], gene silencing [2], and metabolism [3]. They are ubiquitous among all the kingdoms of life and the number of sirtuins varies in different organisms. Until now, seven sirtuins (SIRT1–SIRT7) have been reported in mammals. Sirtuins have a core $NAD^+$-binding domain, and their N- and C-terminal domains may lead to distinct localization, different substrate specificity, and even different enzymatic activities [4], including deacetylation, desuccinylation, demalonylation, glutarylation [5,6], and ADP-ribosylation [7]. It is noteworthy that some sirtuins that had been reported to have undetectable deacetylase activity [7,8] were found to have efficient deacetylases activity. For example, SIRT4 can deacetylate malonyl-CoA decarboxylase (MCD) and, therefore, inhibit its activity [9]. The deacetylase activity of SIRT6 can be largely enhanced by several fatty acids or in the presence of the nucleosome proteins [10,11].

Mono-ADP-ribosylation is a reversible and covalent modification involving the transfer of the ADP–ribose moiety from $NAD^+$ to the substrates, and usually leads to the inhibition of substrate functions.

Among the sirtuins, SIRT4 and SIRT6 were reported to possess ADP-ribosylation activity, and they modify glutamate dehydrogenase (GDH) and poly-ADP-ribose polymerase 1 (PARP1), respectively [7,12]. Mono-ADP-ribosylation often occurs on arginine, cysteine, glutamine, or lysine residues, which can be differentiated by chemical stability assay. For example, $NH_2OH$ can specifically break the ADP–ribosyl–arginine linkage other than linkages with other residues [13–16]. In fact, two kinds of ADP-ribosylation have been reported in prokaryotes. One is the well-defined DraT/DraG system, which is involved in the regulation of nitrogenase activity. In response to a negative stimulus such as the presence of ammonium or a decrease in the available cell energy, DraT can ADP-ribosylate Fe protein which in turn dissociates from MoFe protein and ultimately inhibits the nitrogenase activity, while DraG can remove the ADP–ribose moiety from Fe protein and therefore reactivate the nitrogenase [17,18]. In addition to DraT, some toxins secreted by pathogens also possess ADP-ribosylation activity and can disrupt the essential functions of the host cells [13,16,19]. For example, cholera toxin and pertussis toxin can ADP-ribosylate regulatory G proteins and then interfere with their signal transduction.

Although well characterized in eukaryotes, sirtuins counterparts in prokaryotes remain largely unexplored. Until now, only SIRT5 homologues have been studied in prokaryotes. For example, CobB in *Salmonella* can deacetylate a large number of proteins, including ACS, CheY, GapA, and RcsB, thus regulating metabolism, chemotaxis, and transcription [20–22]. However, whether there are other sirtuin homologues and their possible functions in prokaryotes remains to be determined.

In the present work, a human SIRT4 homologue MSMEG_4620 was identified in *Mycobacterium smegmatis* by *in silico* analysis, and was found to be critical for bacterial growth when grown in 7H9 minimal medium. This is the first report about an SIRT4 homologue in prokaryotes.

## Materials and Methods

### Cloning, over-expression, and purification of proteins

Using the genomic DNA of *M. smegmatis* $mc^2155$ as the template, *MSMEG_4620* was PCR amplified (**Supplementary Table S1**). The PCR products were digested with *Eco*RI and *Hin*dIII (ThermoFisher, Carlsbad, USA) and then cloned into pET28a (Merck Millipore, Billerica, USA) with a 6× His tag at its N terminus. Finally, the plasmid pET28a-*MSMEG_4620* was transformed into competent *Escherichia coli* BL21 (DE3) cells for expression.

Overnight culture was diluted (1 : 100) in fresh LB broth and grown at 37°C until $OD_{600}$ reached 0.7, and then induced at 30°C with 0.1 mM isopropyl β-D-thiogalactoside (IPTG) for 7 h. After that, cells were harvested by centrifugation at 6000 *g* for 10 min, and then re-suspended in buffer A (20 mM Tris–HCl, pH 8.0, 0.5 M NaCl, 10% glycerol, and 20 mM imidazole). The cells were disrupted by ultra-sonication followed by centrifugation at 20,000 *g* for 20 min to remove cell debris. The supernatant was collected and applied to Ni-NTA Sepharose (Qiagen, Hilden, Germany) which was pre-equilibrated with buffer A. Proteins were eluted with buffer B (20 mM Tris–HCl, pH 8.0, 0.5 M NaCl, 10% glycerol, and 40 mM imidazole) and then with buffer C (20 mM Tris–HCl, pH 8.0, 0.5 M NaCl, 10% glycerol, and 500 mM imidazole). Fractions eluted with buffer C were pooled together and dialyzed against buffer D (20 mM Tris–HCl, pH 8.0, 50 mM NaCl, and 20% glycerol). Finally, proteins were concentrated and concentrations were determined by Bradford protein assay.

For the expression of SIRT4 protein, *SIRT4* gene from human cDNA was amplified using primers *SIRT4-Sfu*I-F and *SIRT4-Xho*I-R, and then cloned into pPICZC vector (ThermoFisher, Waltham, USA) for intracellular expression. After that, pPICZC-*SIRT4* was transformed into competent *Pichia pastoris* X33 and recombinants were checked by primers *AOX*-F and *AOX*-R. Finally, a single colony was inoculated into 50 ml medium A (1% yeast extract, 2% peptone, 100 mM potassium phosphate, pH 6.0, 1.34% YNB, $4 \times 10^{-5}$% biotin, and 1% glycerol) and cultured for 3 days at 30°C in a shaker (250 rpm) until $OD_{600}$ reached 5.0. Cells were harvested, transferred to 25 ml fresh medium A and then induced with 1% methanol for 3 days, during which extra 1% methanol was added every 24 h.

### Deacetylase activity assay

Boc-lys(ac)-AMC (BACHEM, Torrance, USA) was used as substrate to determine the $NAD^+$-dependent protein deacetylase activity. The reactions were performed in 96-well plates at 30°C for 3 h in 50 μl sirtuin buffer (50 mM Tris–HCl, pH 8.0, 137 mM NaCl, 2.7 mM KCl, and 1 mM $MgCl_2$) with 600 μM $NAD^+$, 4 μg SIRT enzyme, and 8 μM Boc-lys(ac)-AMC in the presence or absence of fatty acid. The reactions were terminated by incubation with 60 μl of stop solution containing 500 μg/ml trypsin and 10 mM NAM for additional 30 min at 37°C. Finally, the fluorescence was measured by using a micro-plate reader (BioTek, Winooski, USA) with excitation at 390 nm and emission at 460 nm [21].

### Detection of biotin-ADP-ribosylated MSMEG_4620

To detect MSMEG_4620 ADP-ribosylation activity, 50 μM biotinylated NAD (6-biotin-17-NAD; R&D, Minneapolis, USA) was incubated with 50 mM Tris–HCl (pH 7.2), 150 mM NaCl and 2 μg MSMEG_4620 at 25°C for 3 h [13]. The samples were prepared and resolved on sodiumdodecyl sulfate–polyacrylamide gel electrophoresis (SDS–PAGE), transferred onto PVDF membrane. Membranes were blocked by TBS buffer (100 mM Tris–HCl, pH 7.5, and 100 mM NaCl) containing 1% peptone and 10% Tween 20, and then incubated with Avidin–HRP (diluted 1 : 1000 in TBS with 0.1% peptone and 0.5% Tween 20; eBioscience, San Diego, USA) for 2 h at room temperature. Finally, chemiluminescent detection was performed by using the ECL reagent kit (GE Health, Bethesda, USA).

### Site-directed mutagenesis

Site-directed mutagenesis was carried out with KOD-Plus-Neo polymerase (Toyobo, Kita-ku, Japan) using pET28a-*MSMEG_4620* as the template. The primers used in this study are all listed in **Supplementary Table S1**. Mutations of H114Y, S24A, C127A, C262A, and E264Q were confirmed by DNA sequencing and the proteins were purified as described above.

### Chemical stability assay

Two micrograms of MSMEG_4620 was incubated with 50 mM PIPES or Tris–HCl (pH 7.2), 150 mM NaCl, and 50 μM biotin–NAD at 25°C for 3 h. After that, the reaction was terminated by boiling for 5 min, and samples were incubated with 0.5 M NaCl, 10 mM $HgCl_2$, or 2 M $NH_2OH$ for additional 2 h at 30°C [13,23]. Finally, samples were subject to western blot analysis as described above.

### Quantitative real-time PCR

*Mycobacterium smegmatis* cultured in rich or minimal medium at different growth phases were harvested and disrupted by Beadsbeater

(BioSpec Products, Bartlesville, USA), and then RNA samples were extracted using the Trizol Reagent (Ambion, Austin, USA). cDNA was synthesized using the SuperScriptIII First Strand kit (Invitrogen, Carlsbad, USA) with random hexamers as the primers. After that, transcription levels of *MSMEG_4620* and *MSMEG_5175* were measured by qPCR with Applied Biosystems 7500 Fast (Applied Biosystems, Foster City, USA) and the fold changes were normalized to 16S rRNA.

## CD spectrometry

MSMEG_4620 protein was dialyzed against 2 mM Tris–HCl (pH 7.2) and concentrated to 0.2 mg/ml. The CD spectra were measured on a J-715 spectropolarimeter (Jasco, Easton, USA) in the far-ultra-violet region (250–190 nm) in steps of 1 nm, and each spectrum reported was an average of five scans [24].

## Construction of *MSMEG_4620* null mutant in *M. smegmatis* mc$^2$155

The *MSMEG_4620*::*hyg* null mutant (*MSMEG_4620*-KO) was constructed in *M. smegmatis* mc$^2$155 as follows: two homology arms (about 1 kb for left and right arms) of *MSMEG_4620* gene were PCR amplified from genomic DNA by using primers T1-*Xho*I-F/T1-*Spe*I-R and T2-*Spe*I-F/T2-*Kpn*I-R (**Supplementary Table S1**), respectively. After digestion, both T1 and T2 were cloned into pMZ+. The resulted plasmid pMZ-*T1T2* was digested with *Spe*I, followed by ligation with *Spe*I-FRT-*hyg*-FRT-*Spe*I cassette from pCMG50. Then pMZ-T1-*hyg*-T2 was transformed into competent cell of *M. smegmatis* mc$^2$155. Three days later, clones were checked with check-F and -R in the genome, and finally pMN234 plasmid was transformed to remove the *hyg* gene as described previously [25].

## Growth curves

To obtain the growth curves, about 3 days' cultures of *M. smegmatis* and its derivative strains were diluted with 35 ml culture media with appropriate antibiotics to make a starting $OD_{600}$ of about 0.045. Culture media used were LBG broth containing extra 0.05% Tween 80 and 0.5% glycerol, 7H9 broth containing extra 0.05% Tween 80 and 0.5% glycerol, and 7H9 minimal medium. The bacteria was incubated at 37°C and the $OD_{600}$ of the cultures were monitored at interval of indicated hours. When the $OD_{600}$ exceeded 1.0, samples were diluted in order to remain within the linear range of detection.

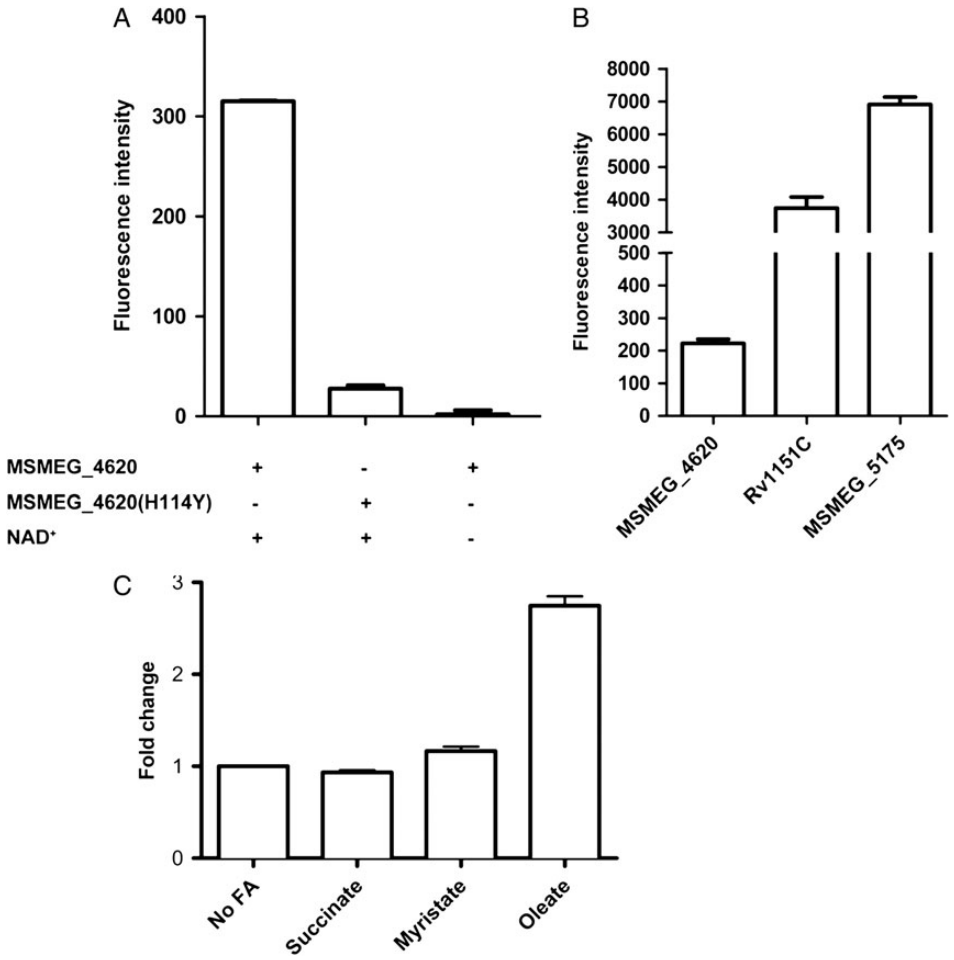


**Figure 1. MSMEG_4620 exhibited weak deacetylase activity that could be activated by fatty acid** (A) MSMEG_4620 possessed deacetylase activity. Purified wild-type MSMEG_4620 and H114Y mutant were incubated with the sirtuin buffer and Boc-lys(ac)-AMC in the presence or absence of $NAD^+$. Fluorescence was measured (390 nm emission and 460 nm excitation). (B) MSMEG_4620 showed much lower deacetylase activity than Rv1151c or MSMEG_5175. Equal amount of MSMEG_4620, Rv1151c, and MSMEG_5175 were added to the reaction and their deacetylase activities were detected as described in (A). (C) The deacetylase activity of MSMEG_4620 could be activated by fatty acid. 100 μM of succinate, myristate, or oleate was added individually to the reaction and deacetylase activity was measured as above.

## Results

### MSMEG_4620 was identified as a SIRT4 homologue by *in silico* analysis

It has been reported that SIRT homologues were widely distributed in the bacteria [20–22]. For example, Rv1151c is capable of deacetylating the acetyl-CoA synthetase from *M. tuberculosis* [26]. In this study, the genome sequence of the model mycobacterial strain *M. smegmatis* was screened by BLASTP, and two SIRT homologues (MSMEG_4620 and MSMEG_5175) were identified. Phylogenetic analysis of SIRT family proteins from bacteria, archaea bacteria, yeast and human showed that MSMEG_4620 and SIRT4 cluster together, while MSMEG_5175 cluster with SIRT5 (**Supplementary Fig. S1**). Specifically, MSMEG_5175 shares 69% and 40% identity with Rv1151c and human SIRT5, respectively, which suggests that it may be an SIRT5 homologue and possess deacetylase activity [11,27] (**Supplementary Fig. S2**). Since MSMEG_4620 is different from Rv1151c (31% identity only) or MSMEG_5175 (29% identity only) based on amino acids sequence, we presume that MSMEG_4620 has activities that is different from the characterized deacetylase MSMEG_5175. Indeed, MSMEG_4620 shares 44% identity and 58% similarity with human SIRT4, and the critical catalytic histidine residue in the 'HG' motif, which is conserved in all known sirtuins, is present in MSMEG_4620. We speculate that MSMEG_4620 is a SIRT4 homologue and it may possess similar enzymatic activities to SIRT4 (**Supplementary Fig. S2**).

### MSMEG_4620 exhibited weak deacetylase activity and could be activated by fatty acid

To test whether MSMEG_4620 possesses deacetylase activity, a fluorogenic substrate Boc-lys(ac)-AMC was used to determine its deacetylase activity [21]. Briefly, trypsin could digest this chemical only when its lysine residue is deacetylated. Upon cleavage by trypsin, the AMC moiety of Boc-lys(ac)-AMC is released and fluorescence is emitted. As the histidine within the catalytic core is a key residue involved in the deacetylase activity among SIRT family proteins [28], the corresponding H114 of MSMEG_4620 was mutated to tyrosine. As shown in **Fig. 1A**, the deacetylase activity of MSMEG_4620 showed an $NAD^+$-dependent

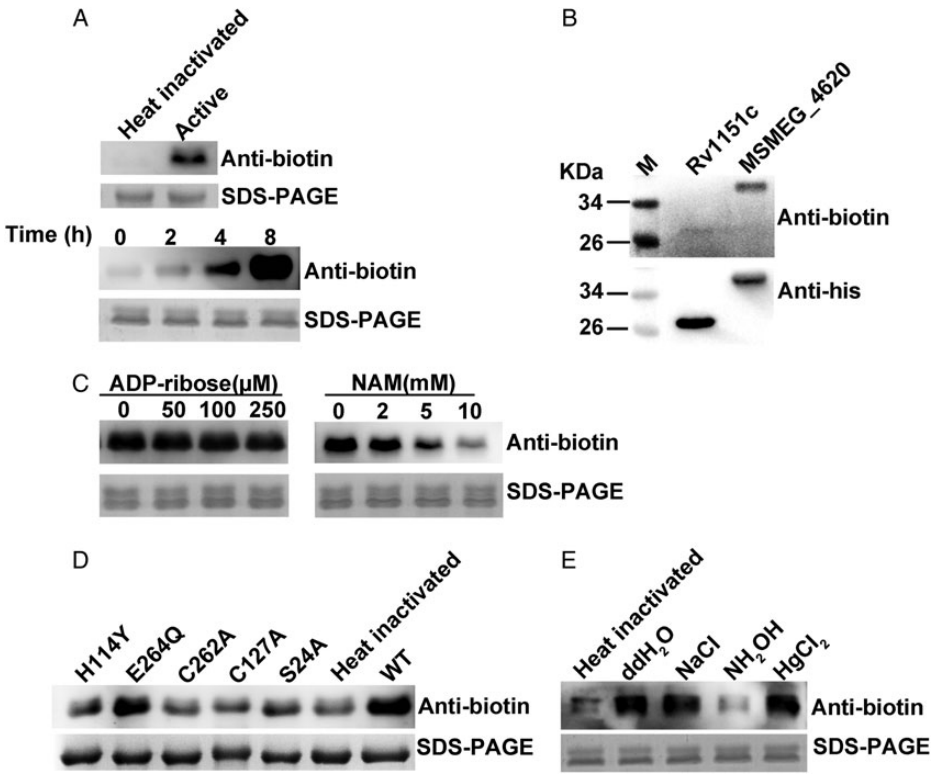


**Figure 2. MSMEG_4620 exhibited auto ADP-ribosyltransferase activity** (A) MSMEG_4620 could be auto ADP-ribosylated in a time-dependent manner. Purified MSMEG_4620 was incubated with 50 mM PIPES (pH 7.2), 150 mM NaCl and 50 μM biotin–NAD for indicated times. For western blot analysis, Avidin–HRP was used to detect the biotin-ADP-ribosylated MSMEG_4620. The loading control was shown in bottom panel. (B) MSMEG_4620 showed higher auto ADP-ribosyltransferase activity than Rv1151c. Purified MSMEG_4620 and Rv1151c were added to the reaction as described in (A), respectively. Avidin–HRP was used to measure the auto ADP-ribosyltransferase activity (the upper panel). Anti-His antibody (the bottom panel) was used to normalize the amount of the two proteins. Positions of molecular mass markers were labeled on the left. (C) Auto ADP-ribosyltransferase activity of MSMEG_4620 was inhibited by NAM, but not ADP–ribose. The reaction mixture containing 50 mM PIPES (pH 7.2), 50 μM biotin–NAD and 2 μg MSMEG_4620 was incubated at 25°C in the presence of indicated concentrations of NAM or ADP–ribose. Avidin–HRP was used to detect the biotin-ADP-ribosylated MSMEG_4620. (D) Mutations of MSMEG_4620 led to a great loss of auto ADP-ribosyltransferase activity. Mutated proteins S24A, H114Y, C127A, C262A, and E264Q were purified in a native form. An equal amount of these proteins was separately added to the reaction mixture containing 50 mM PIPES (pH 7.2) and 50 μM biotin–NAD, using heat-inactivated MSMEG_4620 as a control. After 3 h of incubation, samples were subject to western blot analysis to detect the biotin-ADP-ribosylated MSMEG_4620. (E) Chemical stability assay indicated auto ADP-ribosylation of MSMEG_4620 happened on arginine. MSMEG_4620 (5 μg) was incubated with 50 μM biotin–NAD in the reaction buffer containing 50 mM PIPES (pH 7.2), 150 mM NaCl at 25°C for 3 h. After that, it was divided into aliquots, followed by boiling for 5 min, and then incubated with the indicated chemicals ($ddH_2O$, 0.5 M NaCl, 10 mM $HgCl_2$, or 2 M $NH_2OH$) for two more hours at 30°C. Avidin–HRP was used to detect the biotin-ADP-ribosylated MSMEG_4620, and heat-inactivated MSMEG_4620 was used as a negative control.

manner and H114Y mutation resulted in a nearly complete loss of this activity. But the deacetylase activity of MSMEG_4620 was much lower than that of Rv1151c (5%) or MSMEG_5175 (2.8%) (**Fig. 1B**).

It was reported that the deacetylase activity of SIRT6 could be activated by long-chain fatty acids [11]. So, we further tested whether the deacetylase activity of MSMEG_4620 could also be activated by fatty acids. Three kinds of fatty acids including succinate, myristate and oleate were examined. As shown in **Fig. 1C**, oleate, other than succinate and myristate, could increase the deacetylase activity of MSMEG_4620 by 2.5-fold.

## MSMEG_4620 showed strong ADP-ribosyltransferase activity

We presumed that MSMEG_4620 might not function mainly as deacetylase physiologically because of its very weak deacetylase activity (**Fig. 1B**). It has been reported that, besides its deacetylase activity, SIRT4 also possesses ADP-ribosyltransferase activity [7]; therefore, we also tested whether MSMEG_4620 exhibited ADP-ribosyltransferase activity. Surprisingly, MSMEG_4620 could not ADP-ribosylate histones (data not shown), but it could transfer the biotinylated ADP–ribose to itself in a time-dependent manner (**Fig. 2A**). When compared with Rv1151c, which was reported to possess the auto ADP-ribosyltransferase activity [21], MSMEG_4620 showed a much higher activity (**Fig. 2B**). To rule out the possibility that the auto ADP-ribosylation was due to the non-enzymatic modification of free ADP–ribose [29], we carried out the auto ADP-ribosylation reaction in the presence of ADP–ribose or NAM. As shown in **Fig. 2C**, auto ADP-ribosyltransferase activity of MSMEG_4620 could be inhibited by NAM, but not by ADP–ribose. The optimal pH and temperature for this enzymatic reaction was pH 7.2 and 25°C respectively (**Supplementary Fig. S3**). These results suggested that MSMEG_4620 could ADP-ribosylate itself in an enzymatic-dependent manner.

## Identification of key residues involved in the auto ADP-ribosylation of MSMEG_4620

To get further insight into the molecular basis of the enzymatic auto ADP-ribosyltransferase activity of MSMEG_4620, several highly conserved residues were selected and mutated by site-directed mutagenesis according to multiple sequence alignment (**Supplementary Fig. S1**). Among them, residue Ser-24 was reported to be critical for the ADP-ribosyltransferase activity [8] and residue His-114 was positioned in the core catalytic domain [30]. There are five conserved cysteines in MSMEG_4620, including residues cysteine-122, 127, 178, 181 and 262, the first four of which may be involved in secondary structure maintenance [31]. Only C127A and C262A mutant proteins were successfully purified and therefore applied to the ADP-ribosyltransferase activity examination. As shown in **Fig. 2D**, mutations of S24A, H114Y, C127A, and C262A in MSMEG_4620 led to a great loss of its auto ADP-ribosyltransferase activity. Sequence alignment showed that E264 of MSMEG_4620 is conserved as the residue E381 in *Pseudomonas aeruginosa* ExoS which is a member of the bacterial ADP-ribosylating exotoxin family [32]. However, glutamine substitution of E264 did not affect the auto ADP-ribosyltransferase activity of MSMEG_4620 (**Fig. 2D**).

## Chemical stability assay indicated an arginine–ADP–ribose linkage on MSMEG_4620

ADP-ribosylation usually occurs on arginine, cysteine, and lysine residues [13,23]. To identify the ADP-ribosylated residues of MSMEG_4620, chemical stability experiment was carried out by using $HgCl_2$, $NH_2OH$, or NaCl that could specifically break the bonds between ADP-ribosyl group and cysteine, arginine, or lysine residue, respectively [14,15,23]. The results showed that ADP-ribosyl group could only be removed by $NH_2OH$ treatment (**Fig. 2E**), suggesting that MSMEG_4620 could enzymatically transfer the ADP–ribose moiety to arginine residues. To confirm it, Arg-33 which conserved among sirtuin proteins was mutated and results showed that it led to a remarkable decrease of auto ADP-ribosylation (**Supplementary Fig. S4**).

## Auto ADP-ribosyltransferase activity of MSMEG_4620 could be activated by ferric ion

A previous study showed that $Zn^{2+}$ ion is important for the enzymatic activity of Sir2p [31]. In addition, NarE, an auto ADP-ribosyltransferase from *Neisseria meningitidis*, could bind ferric ion through the Fe-S center, which is crucial for its catalytic activity [23]. In order to test whether MSMEG_4620 could be activated by certain metal ions, $Ca^{2+}$, $Mg^{2+}$, $Fe^{3+}$, $Zn^{2+}$, $Cu^{2+}$ and $Mn^{2+}$ were individually added into the auto ADP-ribosylation reaction system. As shown in **Fig. 3A**, $Fe^{3+}$ greatly increased its auto ADP-ribosyltransferase activity, while $Zn^{2+}$ and $Mg^{2+}$ could also slightly activate it. When EDTA was added to the reaction, auto ADP-ribosylation of MSMEG_4620 was decreased dramatically (**Fig. 3B**). Auto ADP-ribosylation of MSMEG_4620 was elevated with an increase of $Fe^{3+}$ concentration (**Fig. 3C**). We speculated that the activation of auto ADP-ribosyltransferase by $Fe^{3+}$ was due to a secondary structure change upon $Fe^{3+}$ binding. To test this hypothesis, CD spectra analysis was performed with purified MSMEG_4620 in the presence or absence of $Fe^{3+}$. As shown in **Fig. 3D** and **Supplementary Table S2**, $Fe^{3+}$ caused a great secondary structure change in MSMEG_4620, which might contribute to the auto ADP-ribosyltransferase activation.

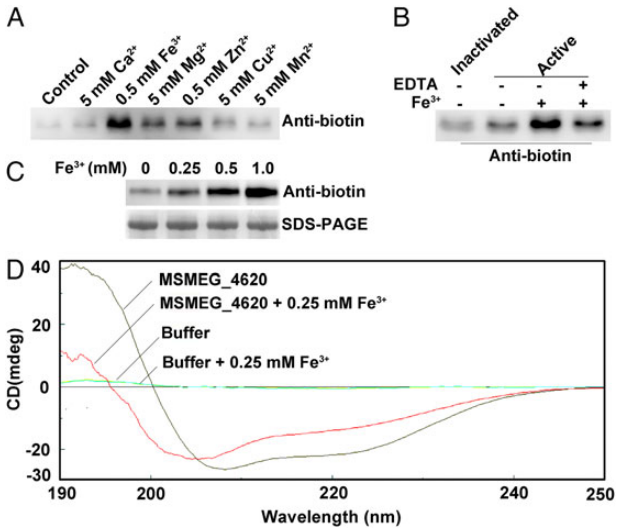


**Figure 3. Auto ADP-ribosyltransferase activity of MSMEG_4620 was activated by ferric ion** (A) Several kinds of ions of indicated concentrations were added to the reaction mixture containing 50 mM Tris–HCl (pH 7.2), and 150 mM NaCl at 25°C for 3 h in the presence or absence of 1 mM EDTA (B) or indicated concentrations of $Fe^{3+}$ (C). Samples were ultimately subject to western blot analysis with Avidin–HRP to detect the biotin-ADP-ribosylated MSMEG_4620. MSMEG_4620 without ion was included as the control. (D) CD spectra analysis of MSMEG_4620 under 0.25 mM $Fe^{3+}$. As described in Materials and Methods section, the CD spectra was measured in the far-ultra-violet region (250–190 nm) in steps of 1 nm. Each spectrum reported here was an average of five scans.

### MSMEG_4620 was essential for mycobacterial growth in natural environments

In order to explore the role of SIRT4 homologues in mycobacterial species, mycobacterial genomic sequences were collected and the distribution of SIRT homologues among them was analyzed. The results showed that pathogenic species tended to possess only one SIRT5 homologue, while non-pathogenic species from natural environments tended to possess both SIRT5 and SIRT4 homologues (**Supplementary Table S3**). For example, *M. smegmatis* possessed a SIRT5 homologue (MSMEG_5175) and a SIRT4 homologue (MSMEG_4620), while *M. tuberculosis* had only one SIRT5 homologue (Rv1151c). This trend suggested that the SIRT4 homologue might play a role in fundamental metabolism and growth of mycobacterial species in the natural environments. To examine this hypothesis, the *MSMEG_4620* null mutant was constructed in *M. smegmatis* mc$^2$155 by homologous recombination. The growth curves of *MSMEG_4620* null mutant in rich or minimal media were compared with that of its parental strain. As shown in **Fig. 4A**, there was no growth difference between the two strains either in relatively rich liquid LBG medium or 7H9 medium with extra glycerol and Tween 80. However, *MSMEG_4620* null mutant exhibited a severe growth defect in the 7H9 minimal medium. Meanwhile, the mRNA level of *MSMEG_4620* increased dramatically when the wild-type strain was grown in the minimal medium other than rich medium (**Fig. 4B**). Instead, the transcription level of *MSMEG_5175* did not show significant changes under the conditions tested.

## Discussion

In this study, a bacterial SIRT4 homologue MSMEG_4620 was identified and characterized. The phylogenetic analysis showed that MSMEG_4620

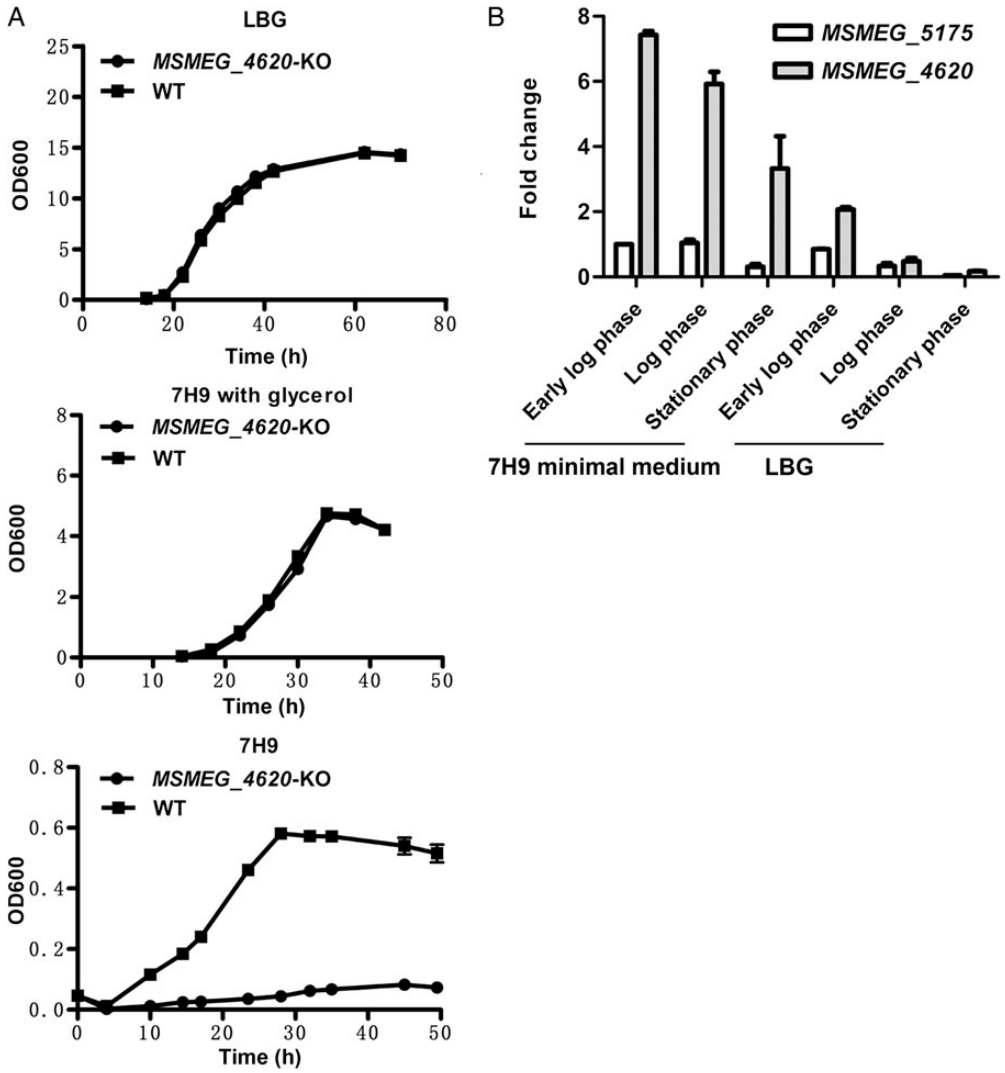


**Figure 4. MSMEG_4620 played a key role in mycobacterial growth in the natural environment** (A) *MSMEG_4620* null mutation (*MSMEG_4620*-KO) in *M. smegmatis* mc$^2$155 led to a growth defect when grown in 7H9 minimal medium. The growth curves of wild-type or *MSMEG_4620*-KO strain in different mediums, including LBG medium, 7H9 minimal medium with/without glycerol, were measured at 37°C. Results were obtained from three independent experiments performed in triplicate. (B) Transcription levels of *MSMEG_4620* and *MSMEG_5175* grown in LBG medium and 7H9 minimal medium were compared. *M. smegmatis* mc$^2$155 grown in these mediums at early log phase, log phase and stationary phase, respectively, were harvested. RNA samples were extracted using the Trizol reagent, followed by cDNA synthesis and ultimately applied to 7500 FAST. The final results of fold increase were normalized to 16S rRNA.

and SIRT4 branch together suggesting that MSMEG_4620 of *M. smegmatis* is an SIRT4 homologue. Although SIRT4 could ADP-ribosylate GDH and inhibited its activity [7], it did not show any detectable auto ADP-ribosyltransferase activity and could not be activated by $Fe^{3+}$ either when compared with MSMEG_4620 (**Supplementary Fig. S5**). Undetectable deacetylase activity was found in human SIRT4 [7,33], while its homologue MSMEG_4620 was found to be an $NAD^+$-dependent deacetylase, although with much lower activity than Rv1151c and MSMEG_5175, both of which were efficient deacetylases [21,26]. This might be explained by the different substrates used in these studies, i.e. Fluor de Lys substrate and chemically acetylated histone peptide, respectively, and probably, SIRT4 could only recognize and deacetylate its stringent substrates such as malonyl-CoA decarboxylase (MCD) [9]. To explore the function of MSMEG_4620, its physiological substrates need to be investigated in the future.

SIRT4 is active under nutrient-replete conditions to repress fatty acid oxidation while promoting lipid anabolism by deacetylating and inhibiting malonyl CoA decarboxylase (MCD) [9]. Similarly, the deacetylase activity of MSMEG_4620 could be activated by fatty acid. Oleate, one of the tested fatty acids, exhibited about 2.5-fold increase of deacetylase activity of MSMEG_4620. More fatty acid activators should be tested in the future. As we know, fatty acid biosynthesis plays an important role in building the cell wall of mycobacteria [34], for example, *M. tuberculosis* has about 250 genes involved in the fatty acid metabolism [35]. We speculated that the deacetylase activity of MSMEG_4620 could be activated by fatty acids *in vivo*, which played important roles in mycobacterial physiological processes. Meanwhile, MSMEG_4620 was also found to be an auto ADP-ribosyltransferase with much higher activity than Rv1151c, and could be activated by some metal ions such as $Fe^{3+}$, $Mg^{2+}$, and $Zn^{2+}$. CD spectra analysis showed that the addition of $Fe^{3+}$ led to a secondary structural change in MSMEG_4620, which might contribute to its activation. Since mycobacterial species acquire these metal ions through different ways to maintain their homeostasis *in vivo*, such as ABC-zinc transporter system, transporter protein MgtC, and iron chelators mycobactins, their activation of MSMEG_4620 may be associated with its physiological roles in the ion homeostasis.

Despite the unknown substrates of MSMEG_4620, our data support that it plays a critical role in the growth of *M. smegmatis*. When grown in the minimal medium, such as 7H9 minimal medium which contains sodium citrate as the carbon source, *MSMEG_4620* null mutant had severe growth defect. Based on this observation, we believe that MSMEG_4620 plays a pivotal role when *M. smegmatis* runs out of nutrients. *Mycobacterium smegmatis* up-regulated the transcription level of *MSMEG_4620* to adapt itself to the malnutrition stress, while the *MSMEG_4620* null mutant could never be compensated, which led to the growth retardation. From the perspective of evolution, the fact that SIRT4 homologues exist only in the enviromental mycobacterial species indicates that they may be important for the fundamental metabolism of these species under malnutrition. Non-pathogenic mycobacterial species usually grow in wild environment and are frequently lack of nutrients. On the contrary, pathogenic mycobacterial species may survive by acquisition of certain nutrients like carbon sources, amino acids, fatty acids, and essential metal ions from host cells. This may explain why pathogenic mycobacterial species gradually lost the SIRT4 homologue during evolution, while non-pathogenic species still heavily rely on it.

## Supplementary Data

Supplementary data is available at *ABBS* online.

## Funding

This work was supported by grants from the State Key Development Programs for Basic Research of China (No. 2015CB554203), the National Natural Science Foundation of China (Nos. 31270173 and 31070114), and the Program for Professor of Special Appointment (Eastern Scholar) at Shanghai Institutions of Higher Learning.

## References

1. Wood JG, Rogina B, Lavu S, Howitz K, Helfand SL, Tatar M, Sinclair D. Sirtuin activators mimic caloric restriction and delay ageing in metazoans. *Nature* 2004, 430: 686–689.
2. Vaquero A, Scher M, Erdjument-Bromage H, Tempst P, Serrano L, Reinberg D. SIRT1 regulates the histone methyl-transferase SUV39H1 during heterochromatin formation. *Nature* 2007, 450: 440–444.
3. Schwer B, Verdin E. Conserved metabolic regulatory functions of sirtuins. *Cell Metab* 2008, 7: 104–112.
4. Flick F, Luscher B. Regulation of sirtuin function by posttranslational modifications. *Front Pharmacol* 2012, 3: 29.
5. Du J, Zhou Y, Su X, Yu JJ, Khan S, Jiang H, Kim J, *et al*. Sirt5 is a NAD-dependent protein lysine demalonylase and desuccinylase. *Science* 2011, 334: 806–809.
6. Tan M, Peng C, Anderson KA, Chhoy P, Xie Z, Dai L, Park J, *et al*. Lysine glutarylation is a protein posttranslational modification regulated by SIRT5. *Cell Metab* 2014, 19: 605–617.
7. Haigis MC, Mostoslavsky R, Haigis KM, Fahie K, Christodoulou DC, Murphy AJ, Valenzuela DM, *et al*. SIRT4 inhibits glutamate dehydrogenase and opposes the effects of calorie restriction in pancreatic beta cells. *Cell* 2006, 126: 941–954.
8. Liszt G, Ford E, Kurtev M, Guarente L. Mouse Sir2 homolog SIRT6 is a nuclear ADP-ribosyltransferase. *J Biol Chem* 2005, 280: 21313–21320.
9. Laurent G, German NJ, Saha AK, de Boer VC, Davies M, Koves TR, Dephoure N, *et al*. SIRT4 coordinates the balance between lipid synthesis and catabolism by repressing malonyl CoA decarboxylase. *Mol Cell* 2013, 50: 686–698.
10. Gil R, Barth S, Kanfi Y, Cohen HY. SIRT6 exhibits nucleosome-dependent deacetylase activity. *Nucleic Acids Res* 2013, 41: 8537–8545.
11. Feldman JL, Baeza J, Denu JM. Activation of the protein deacetylase SIRT6 by long-chain fatty acids and widespread deacylation by mammalian sirtuins. *J Biol Chem* 2013, 288: 31350–31356.
12. Mao Z, Hine C, Tian X, Van Meter M, Au M, Vaidya A, Seluanov A, *et al*. SIRT6 promotes DNA repair under stress by activating PARP1. *Science* 2011, 332: 1443–1446.
13. Icenogle LM, Hengel SM, Coye LH, Streifel A, Collins CM, Goodlett DR, Moseley SL. Molecular and biological characterization of Streptococcal SpyA-mediated ADP-ribosylation of intermediate filament protein vimentin. *J Biol Chem* 2012, 287: 21481–21491.
14. Cervantes-Laurean D, Minter DE, Jacobson EL, Jacobson MK. Protein glycation by ADP-ribose: studies of model conjugates. *Biochemistry* 1993, 32: 1528–1534.
15. Cervantes-Laurean D, Loflin PT, Minter DE, Jacobson EL, Jacobson MK. Protein modification by ADP-ribose via acid-labile linkages. *J Biol Chem* 1995, 270: 7929–7936.
16. Meyer T, Koch R, Fanick W, Hilz H. ADP-ribosyl proteins formed by pertussis toxin are specifically cleaved by mercury ions. *Biol Chem Hoppe-Seyler* 1988, 369: 579–583.
17. Huergo LF, Souza EM, Araujo MS, Pedrosa FO, Chubatsu LS, Steffens MB, Merrick M. ADP-ribosylation of dinitrogenase reductase in *Azospirillum brasilense* is regulated by AmtB-dependent membrane sequestration of DraG. *Mol Microbiol* 2006, 59: 326–337.
18. Oetjen J, Reinhold-Hurek B. Characterization of the DraT/DraG system for posttranslational regulation of nitrogenase in the endophytic betaproteobacterium *Azoarcus* sp. strain BH72. *J Bacteriol* 2009, 191: 3726–3735.
19. Aktories K, Barmann M, Ohishi I, Tsuyama S, Jakobs KH, Habermann E. Botulinum C2 toxin ADP-ribosylates actin. *Nature* 1986, 322: 390–392.

20. Thao S, Escalante-Semerena JC. Control of protein function by reversible Nvarepsilon-lysine acetylation in bacteria. *Curr Opin Microbiol* 2011, 14: 200–204.
21. Gu J, Deng JY, Li R, Wei H, Zhang Z, Zhou Y, Zhang Y, *et al*. Cloning and characterization of NAD-dependent protein deacetylase (Rv1151c) from *Mycobacterium tuberculosis*. *Biochemistry (Mosc)* 2009, 74: 743–748.
22. Li R, Gu J, Chen YY, Xiao CL, Wang LW, Zhang ZP, Bi LJ, *et al*. CobB regulates *Escherichia coli* chemotaxis by deacetylating the response regulator CheY. *Mol Microbiol* 2010, 76: 1162–1174.
23. Picchianti M, Del Vecchio M, Di Marcello F, Biagini M, Veggi D, Norais N, Rappuoli R, *et al*. Auto ADP-ribosylation of NarE, a *Neisseria meningitidis* ADP-ribosyltransferase, regulates its catalytic activities. *FASEB J* 2013, 27: 4723–4730.
24. Lu LD, Sun Q, Fan XY, Zhong Y, Yao YF, Zhao GP. Mycobacterial MazG is a novel NTP pyrophosphohydrolase involved in oxidative stress response. *J Biol Chem* 2010, 285: 28076–28085.
25. Stephan J, Stemmer V, Niederweis M. Consecutive gene deletions in *Mycobacterium smegmatis* using the yeast FLP recombinase. *Gene* 2004, 343: 181–190.
26. Xu H, Hegde SS, Blanchard JS. Reversible acetylation and inactivation of *Mycobacterium tuberculosis* acetyl-CoA synthetase is dependent on cAMP. *Biochemistry* 2011, 50: 5883–5892.
27. Nakagawa T, Lomb DJ, Haigis MC, Guarente L. SIRT5 Deacetylates carbamoyl phosphate synthetase 1 and regulates the urea cycle. *Cell* 2009, 137: 560–570.
28. Kim HS, Vassilopoulos A, Wang RH, Lahusen T, Xiao Z, Xu X, Li C, *et al*. SIRT2 maintains genome integrity and suppresses tumorigenesis through regulating APC/C activity. *Cancer Cell* 2011, 20: 487–499.
29. Du J, Jiang H, Lin H. Investigating the ADP-ribosyltransferase activity of sirtuins with NAD analogues and $^{32}$P-NAD. *Biochemistry* 2009, 48: 2878–2890.
30. Tanny JC, Dowd GJ, Huang J, Hilz H, Moazed D. An enzymatic activity in the yeast Sir2 protein that is essential for gene silencing. *Cell* 1999, 99: 735–745.
31. Chakrabarty SP, Balaram H. Reversible binding of zinc in *Plasmodium falciparum* Sir2: structure and activity of the apoenzyme. *Biochim Biophys Acta* 2010, 1804: 1743–1750.
32. Liu S, Kulich SM, Barbieri JT. Identification of glutamic acid 381 as a candidate active site residue of *Pseudomonas aeruginosa* exoenzyme S. *Biochemistry* 1996, 35: 2754–2758.
33. Verdin E, Dequiedt F, Fischle W, Frye R, Marshall B, North B. Measurement of mammalian histone deacetylase activity. *Method Enzymol* 2004, 377: 180–196.
34. Zimhony O, Cox JS, Welch JT, Vilcheze C, Jacobs WR Jr. Pyrazinamide inhibits the eukaryotic-like fatty acid synthetase I (FASI) of *Mycobacterium tuberculosis*. *Nat Med* 2000, 6: 1043–1047.
35. Kinsella RJ, Fitzpatrick DA, Creevey CJ, McInerney JO. Fatty acid biosynthesis in *Mycobacterium tuberculosis*: lateral gene transfer, adaptive evolution, and gene duplication. *Proc Natl Acad Sci USA* 2003, 100: 10320–10325.